Formation of Split Electron Paramagnetic Resonance Signals in Photosystem II Suggests That Tyrosine Z Can Be Photooxidized at 5 K in the S 0 and S 1 States of the Oxygen−Evolving C...

2 AUTHORS, INCLUDING:

Chunxi Zhang
Chinese Academy of Sciences

35 PUBLICATIONS   **451** CITATIONS

Formation of Split Electron Paramagnetic Resonance Signals in Photosystem II Suggests That Tyrosine$_Z$ Can Be Photooxidized at 5 K in the S$_0$ and S$_1$ States of the Oxygen-Evolving Complex[†]

Chunxi Zhang[‡] and Stenbjörn Styring*

Department of Biochemistry, Center for Chemistry and Chemical Engineering, P.O. Box 124, Lund University, S-221 00 Lund, Sweden

ABSTRACT: The effect of illumination at 5 K of photosystem II in different S-states was investigated with EPR spectroscopy. Two split radical EPR signals around $g \approx 2.0$ were observed from samples given 0 and 3 flashes, respectively. The signal from the 0-flash sample was narrow, with a width of ~80 G, in which the low-field peak can be distinguished. This signal oscillated with the S$_1$ state in the sample. The signal from the 3-flash sample was broad, with a symmetric shape of ~160 G width from peak to trough. This signal varied with the concentration of the S$_0$ state in the sample. Both signals are assigned to arise from the donor side of PSII. Both signals relaxed fast, were formed within 10 ms after a flash, and decayed with half-times at 5 K of 3−4 min. The signal in the S$_0$ state closely resembles split radical signals, originating from magnetic interaction between Y$_Z^{\bullet}$ and the S$_2$ state, that were first observed in Ca^{2+}-depleted photosystem II samples. Therefore, we assign this signal to Y$_Z^{\bullet}$ in magnetic interaction with the S$_0$ state, Y$_Z^{\bullet}$S$_0$. The other signal is assigned to the magnetic interaction between Y$_Z^{\bullet}$ and the S$_1$ state, Y$_Z^{\bullet}$S$_1$. An important implication is that Y$_Z$ can be oxidized at 5 K in the S$_0$ and S$_1$ states. Oxidation of Y$_Z$ involves deprotonation of the tyrosine. This is restricted at 5 K, and we therefore suggest that the phenolic proton of Y$_Z$ is involved in a low-barrier hydrogen bond. This is an unusually short hydrogen bond in which proton movement at very low temperatures can occur.

Photosynthetic water oxidation to molecular oxygen is a unique function of the photosystem II (PSII)[1] reaction center. PSII is a large protein−cofactor complex, located in the thylakoid membrane. The structure of PSII was recently solved and revealed the gross structural features of the core proteins and the many redox cofactors involved (*1, 2*). Upon illumination, the primary electron donor in PSII, P$_{680}$, donates an electron to the primary pheophytin electron acceptor (Pheo). Pheo$^{-\bullet}$ then delivers the electron to the secondary quinone acceptors, Q$_A$ and Q$_B$. P$_{680}^{+\bullet}$ is very oxidizing (~1.1 eV) and provides the driving force for water oxidation at the donor side of PSII (*3−7*).

The water oxidizing chemistry is catalyzed by the catalytic center located at the lumenal periphery of PSII. It is composed of a cluster of four Mn ions, a Ca^{2+} ion, and a Cl$^-$ ion. The Mn cluster is coordinated by amino acid ligands mainly provided by the D$_1$ protein. The oxidation of two water molecules to molecular oxygen is carried out in a cyclic reaction, the S-cycle, that involves five intermediate redox states, denoted as S$_n$ states ($n = 0−4$). The S$_0$ state is the most reduced state of the Mn cluster. The S$_1$ state is the dark stable state. The S$_2$ and S$_3$ states are more oxidizing and less stable. Oxygen is released in the S$_3$−[S$_4$]−S$_0$ transition which involves the transient S$_4$ state (*8−10*).

The interfacing of the one-electron primary charge separation process with the four-electron water oxidation reaction is a key issue for function of PSII and is also of interest for researchers in other fields (*11*). In PSII, the side chain of D$_1$-Tyr$_{161}$ (named Y$_Z$) plays this interfacing role (*12, 13*). During catalysis, Y$_Z$ delivers one electron to P$_{680}^{+\bullet}$. The result is the formation of the neutral Y$_Z^{\bullet}$ radical. Y$_Z^{\bullet}$ is then reduced by the Mn cluster. Biochemical and structural modeling studies indicate that D$_1$-His$_{190}$ might participate in a H-bond with Y$_Z$, facilitating the oxidation of Y$_Z$ (*14−19*). Symmetrically located to the Y$_Z$ residue, there is another redox-active tyrosine residue on the D$_2$ protein in PSII, denoted Y$_D$. Y$_D$ directly interacts with D$_2$-His$_{189}$, analogous to D$_1$-His$_{190}$, through a H-bond (*20−22*). Both Y$_D$ and Y$_Z$ are oxidized by P$_{680}^{+\bullet}$ and form the neutral Y$^{\bullet}$ radicals (*12, 13, 23*). Y$_Z$ participates in steady-state electron transfer, while Y$_D^{\bullet}$, once formed, is not reduced again. It is in fact one of the most long-lived, natural radicals known.

[1] Abbreviations: Car, β-carotene; Chl, chlorophyll; Cyt b_{559}, cytochrome b-559; EPR, electron paramagnetic resonance; EDTA, ethylendiaminetetraacetic acid; LBHB, low-barrier hydrogen bond; MES, 4-morpholineethanesulfonic acid; P$_{680}$, the primary electron donor of PSII; Pheo, pheophytin; PPBQ, p-phenylbenzoquinone; PSII, photosystem II; Q$_A$ and Q$_B$, primary and secondary quinone electron acceptors; OEC, oxygen-evolving complex; Tris, tris(hydroxymethyl)-aminomethane; Y$_D$, tyrosine 160 on the D$_2$ protein; Y$_Z$, tyrosine 161 on the D$_1$ protein.

The oxidation of Y_Z by $P_{680}^{+\bullet}$ occurs in the nanosecond time scale, and $Y_Z^\bullet$ is reduced by the Mn cluster in the micro-millisecond time scale in active PSII. In many inhibited PSII samples (such as PSII deprived of Mn, Ca^{2+}, or Cl^- or treated by ammonia, acetate, fluoride, or OH^-) (24−44), $Y_Z^\bullet$ is more long-lived and can be trapped by freezing to 77 K during or quickly after illumination at temperatures between 250 and 293 K. Therefore, most studies of $Y_Z^\bullet$ have been performed in variously inhibited samples. $Y_Z^\bullet$ induced in Ca-depleted or acetate-inhibited PSII has been studied in detail. In this system, the strong magnetic coupling between the $Y_Z^\bullet$ and the $S = {}^1\!/_2$ spin of the Mn cluster in the S_2 state gives rise to a broad split EPR signal at $g \approx 2$ (90−250 G wide, depending on the treatment of the samples and measurement conditions). This split EPR signal from $Y_Z^\bullet S_2$ has been used to study the structural relationship between Y_Z and the Mn cluster. The distance between the magnetic centers of Y_Z and the Mn cluster has been estimated to be 7−11 Å (40−42), which is consistent with the distance revealed by the X-ray structure of PSII (1, 2).

Unfortunately, the resolution of the present X-ray structure of PSII is too low to permit absolute molecular knowledge about the environment of Y_Z and the Mn cluster. Therefore, most of the molecular information about $Y_Z^\bullet$ and Y_Z has been deduced from inhibited PSII, which lacks oxygen evolution. It is likely that many of these treatments actually modify the environment and the function of Y_Z (12, 13, 45). Accordingly, there are many unclear features in how Y_Z performs its function in active PSII and how it interacts with the Mn cluster. In particular, very little is known about changes or modifications in these interactions depending on the S-states.

The catalytic water oxidation is blocked below ∼200 K (46−48). In contrast, the primary charge separation can still occur at extremely low temperature (<5 K) to form $P_{680}^{+\bullet}$ and $Q_A^{-\bullet}$. The unstable $P_{680}^{+\bullet}$ is normally reduced by recombination with $Q_A^{-\bullet}$, but it can retrieve an electron from one of several other components in the neighborhood. In particular, a pathway involving a carotenoid (Car), a special chlorophyll denoted Chl$_Z$, and Cyt b_{559} has been well described (49−56).

For long, it was thought that no Y_Z oxidation could occur at liquid helium temperatures. This changed recently, and induction at very low temperature of split radical EPR signals, proposed to originate from $Y_Z^\bullet$ in magnetic interaction with the Mn cluster, was described (57).

Here we study these recently discovered split EPR signals in further detail. We use PSII samples that have been exposed to various numbers of flashes at room temperature. Thereby, we are able to study the effect of illumination at 5 K in different S-states. The formation of split EPR signals during illumination at 5 K is observed only from the S_0 and S_1 states of the Mn cluster. The characteristics and formation processes of these signals at liquid helium temperature offer a new pathway to probe the function of Y_Z in active PSII, and furthermore, it also provides new insight in the mechanism of water oxidation by the Mn cluster.

MATERIALS AND METHODS

PSII-enriched membranes (BBY particles) were prepared from spinach grown on liquid culture medium as in refs 58 and 59. The PSII membranes were dissolved in a medium containing 400 mM sucrose, 15 mM NaCl, 5 mM MgCl$_2$, 5 mM CaCl$_2$, 1 mM EDTA, and 50 mM MES/NaOH (pH = 6.0) and were frozen in liquid nitrogen and stored at −80 °C. The chlorophyll concentration was determined according to ref 60. The rate of oxygen evolution measured using a Clark-type oxygen electrode was 400−500 μmol of O_2 (mg of Chl)$^{-1}$ h^{-1} assayed in saturating white light at 25 °C with 1 mM PPBQ as the external electron acceptor, which is similar to that in ref 59. The samples were always kept in darkness except when otherwise noted.

PSII, with the OEC in the different S-states, was prepared as follows: The samples were thawed and washed with a buffer containing 400 mM sucrose, 15 mM NaCl, 5 mM MgCl$_2$, 5 mM CaCl$_2$, 2 mM EDTA, and 25 mM MES/NaOH (pH = 6.5). Then they were washed once with the same buffer without EDTA. The samples were finally resuspended in the same buffer without EDTA and filled into calibrated EPR tubes. The final concentration was about 2.5−3.0 mg of Chl/mL. All procedures were carried out in the dark or under dim green light at 4 °C, and the samples were kept on ice for at least 30 min.

To synchronize all PSII in the $Y_D^\bullet S_1$ state (46, 61, 62), one preflash was given to the sample after 1 min incubation at room temperature. The preflash was followed by 12 min dark adaptation at room temperature. Then, PPBQ (from a fresh 50 mM solution in DMSO) was added to a final concentration of 1 mM. One minute after the addition of PPBQ, the sample was exposed to various numbers of saturating laser flashes (6 ns, 532 nm, 350 mJ) at 5 Hz provided by an Nd:YAG laser (Spectra Physics) at room temperature. Then the sample was frozen within 1−2 s, first in dry ice/ethanol and then in liquid nitrogen. The EPR measurements on these samples were performed the next day. This procedure resulted in samples where Y_D was oxidized in more than 98% of the PSII centers (46, 61, 62).

The Mn-depleted PSII sample was prepared by Tris washing according to ref 63. The Tris-washed membranes were resuspended in a buffer containing 400 mM sucrose, 15 mM NaCl, 5 mM MgCl$_2$, 5 mM CaCl$_2$, and 25 mM MES/NaOH (pH = 6.5). The final EPR samples (∼3 mg of Chl/mL) were in the same buffer, and 1 mM PPBQ was added before freezing to 77 K.

Ca^{2+}-depleted PSII was prepared according to ref 25. The Ca^{2+}-depleted PSII samples were kept in a buffer containing 400 mM sucrose, 15 mM NaCl, 5 mM MgCl$_2$, and 25 mM MES/NaOH (pH = 6.5) with a concentration of 2.5−3.0 mg of Chl/mL. The samples were given 3 min of room light illumination to induce the stable S_2 state; thereafter, they were kept in the dark on ice for 1 h. PPBQ (1 mM) was added before freezing to 77 K.

Continuous illumination at 0 °C was performed by using a 1000 W projector lamp, using a 5 cm thick filter of CuSO$_4$−water solution to cut off near-IR light (>700 nm). The sample, which was immersed in ice/water (0 °C), was illuminated for 5−10 s followed by rapid freezing in liquid nitrogen. The same setup was used for illumination at 77 K, except that the dewar then contained liquid N_2.

Illumination at liquid helium temperature (5 K) was carried out directly in the EPR cavity using a projector and a plastic light guide. The light was provided by a 150 W projector lamp using a 5 cm thick CuSO$_4$−water solution to cut off
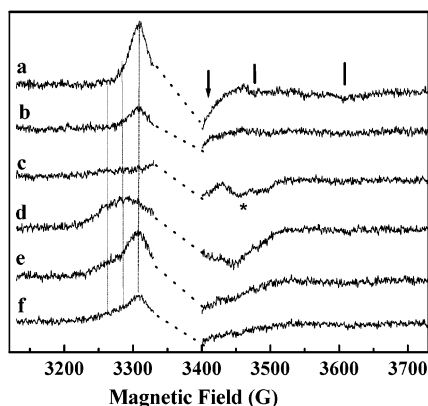
FIGURE 1: Difference EPR spectra recorded at 5 K (spectra recorded during illumination minus spectra recorded before illumination at 5 K) from PSII samples given 0 flash (a), 1 flash (b), 2 flashes (c), 3 flashes (d), 4 flashes (e), and 5 flashes (f). EPR conditions: microwave power, 25 mW; microwave frequency, 9.46 GHz; modulation amplitude, 10 G; temperature, 5 K. The region around the big radical spectrum from $Y_D^•$ is omitted for clarity. The arrow indicates what is probably the high-field part of the new signal in the S_1 state, the bars indicate spectral species probably arising from $Q_A^{-•}Fe^{2+}$, and the asterisk indicates an EPR signal belonging to the S_3 state. The lines indicate the field positions used in Figure 3.

the longer wavelengths (>700 nm). The light intensity, focused on the sample position through the light guide, was about 30 W/m². The light intensity was found to be critical and was controlled in each experiment.

For EPR studies of the flash-induced kinetics of the EPR signals, the exciting laser flashes (6 ns, 532 nm, 10−20 mJ) were provided directly into the EPR cavity.

Low-temperature continuous-wave EPR spectra and kinetics were recorded on a Bruker ELEXYS E580 spectrometer equipped with an Oxford-900 liquid helium cryostat and ITC-503 temperature controller (Oxford Instruments Ltd.). A Bruker ST4102 standard cavity was used for all the measurements. Spectrometer settings are given in the figure legends.

RESULTS

Induction of Two New Split Signals from the S_1 and S_0 States, Respectively. It is well established that the oxidation of the Mn cluster in the S_1 state is blocked at temperatures below ∼77 K (46−48). It is also well-known that illumination of PSII at liquid helium temperatures results in sequential oxidation of donors in the Car/Chl$_Z$/Cyt b_{559} pathway (49−56). In contrast, the possibilities to oxidize Y_Z in different S-states of the OEC at extremely low temperature have not been thoroughly investigated although recent results indicate this to be the case (57). We investigated this in a series of experiments.

First, PSII-enriched membranes were fully synchronized in the $Y_D^•S_1$ state (>98% oxidized Y_D) with a preflash protocol (46, 61, 62). Then PSII was exposed to 0−5 saturating laser flashes and rapidly frozen. Thereby, we had samples enriched in the S_1 (0 and 4 flashes), S_2 (1 and 5 flashes), S_3 (2 flashes), and S_0 state (3 flashes). The samples were then exposed to a short illumination at 5 K.

Figure 1 displays the difference EPR spectra of the spectrum recorded during illumination minus the spectrum recorded before illumination at 5 K for the 0−5 flash PSII samples. Figure 1a is obtained in the 0-flash sample. It displays an EPR signal, in which one peak at the low-field

side (3310 G) of the large spectrum from $Y_D^•$ can be observed very well. No clear peak at the high-field side can be distinguished, although there does exist some absorption at higher magnetic field (see arrow mark in Figure 1a). This signal is similar to a signal first observed by Nugent and Evans (64) and recently assigned to $Y_Z^•$ or $Car^{+•}$ in magnetic interaction with the S_1 state (57). In our 0-flash sample, all PSII centers were in the S_1 state; thus we agree that this new EPR signal is induced from PSII in the S_1 state of the OEC. This is further corroborated by the EPR spectrum recorded in the 1-flash sample (Figure 1b). Here, a similar peak at the same position (3310 G) appeared, but the amplitude decreased to about one-third, which is reasonable since most of the PSII centers had advanced to the S_2 state (see below). The amplitude decreased further to close to zero in the 2-flash sample (Figure 1c).

Figure 1d shows the difference spectrum recorded in the 3-flash sample, which is dominated by the S_0 state (S_0 in ca. 60% of the centers; see below). A new wider EPR signal was observed. Two peaks at low field and high field are clearly observable, and the separation between the two peaks is about 160 G. We assign this new signal to arise from the PSII centers in the S_0 state. This signal is reminiscent of some of the $Y_Z^•S_2$ split signals observed in various inhibited PSII samples.

Figure 1e shows the difference spectrum from the 4-flash sample. In this sample, a large fraction of the PSII centers has returned to the S_1 state. It is therefore not surprising that the peak at 3310 G that is similar to that in the 0-flash sample (compare Figure 1a) comes back. In addition, two shoulder absorptions located at the two low and high magnetic field sides of $g \approx 2$ are observable. These obviously correspond to the broad and symmetric split signal observed in the 3-flash sample (see Figure 1d), but of less intensity. Therefore, the spectrum in Figure 1e recorded in a 4-flash sample is a mixture of the two EPR signals observed in the 0-flash and 3-flash spectra in Figure 1a,d. One signal is narrow and probably asymmetric and originates from the S_1 state (Figure 1a; see below); the other is broad and symmetric and originates from the S_0 state (Figure 1d).

The spectrum recorded in the 5-flash sample is shown in Figure 1f. It is similar to that from the 4-flash sample, but the amplitudes of the new EPR signals decrease further. This spectrum can again be assigned to a mixture of the two split signals in Figure 1a,d but in a different ratio (see below) as compared to the spectrum in the 4-flash sample.

In some of the spectra in Figure 1, there are very weak, light-induced signals at ∼3470 and ∼3610 G (indicated with bars in the figure). These signals somewhat resemble EPR spectra from $Q_A^{-•}$ in magnetic interaction with Fe^{2+} on the acceptor side of PSII (it is called the $Q_A^{-•}Fe^{2+}$ signal) (65). Due to the low concentration of PSII and the presence of PPBQ in our samples (66), the signal is very small. It is therefore difficult to determine the fraction of $Q_A^{-•}$ obtained in the experiment with precision.

Car, Chl$_Z$, and/or Cyt b_{559} are normally oxidized by illumination at low temperature when the Mn cluster is inactive (49−56). It was therefore necessary to control if these components were oxidized by our illumination regime. Oxidation of Cyt b_{559} seems not to have occurred during our illumination by the weak light. This is revealed by the amplitude of the g_z peak from the oxidized cytochrome,
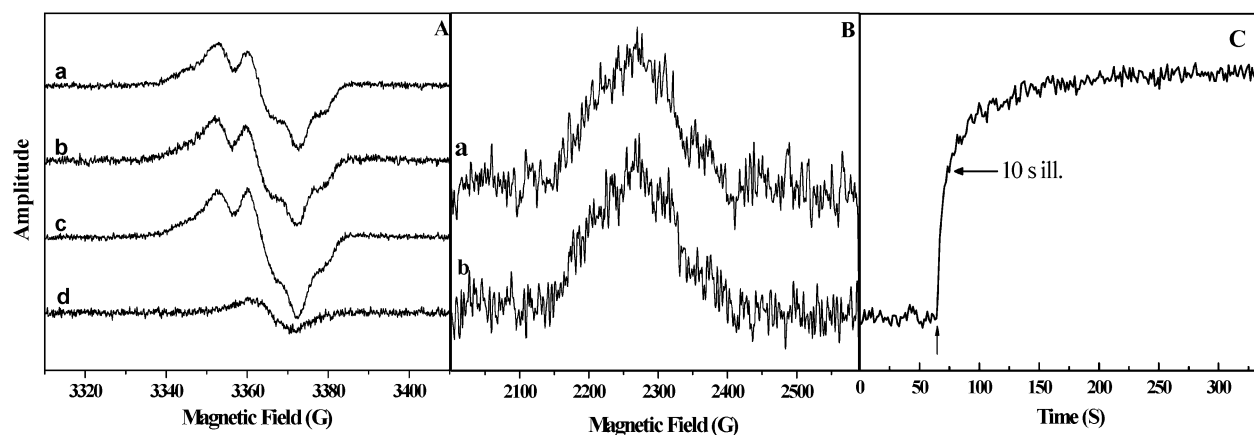
FIGURE 2: EPR spectra of the radical region (A) and Cyt b_{559} (B) and induction kinetics of the EPR signal at 3290 G (see Figure 1d) in the 3-flash samples (C). (A) The radical region of the EPR spectrum in a sample similar to the 3-flash sample in Figure 1d. Spectrum a was recorded prior to the illumination at 5 K. It contains a pure signal from $Y_D^{\bullet}$. Spectrum b was recorded immediately after 10 s illumination at 5 K and shows that there was no induction of a narrow radical signal from Car and/or Chl$_Z$ radicals. Spectrum c was recorded after 4.5 min illumination at 5 K and shows that this prolonged illumination results in formation of a narrow radical species originating from Car and/or Chl$_Z$ radicals. Spectrum d is a difference spectrum obtained by subtracting spectrum a from spectrum c. It shows the pure spectrum of the radical species induced by the prolonged illumination. In this experiment this radical was formed in ca. 10% of the PSII centers. EPR conditions: temperature, 5 K; microwave frequency, 9.46 GHz; modulation amplitude, 3 G; microwave power, 0.5 μW (this power was verified to be nonsaturating for all the radical species studied). (B) The g_z peak of Cyt b_{559} in a similar 3-flash sample as used in (A). Spectrum a shows the spectrum recorded in the dark. Spectrum b was recorded after 4.5 min illumination. The spectra had to be recorded swiftly to avoid decay of the light-induced split signals; hence the signal-to-noise ratio is low. EPR conditions: temperature, 15 K; microwave frequency, 9.46 GHz; modulation amplitude, 10 G; microwave power, 5 mW; time constant, 20 ms. (C) Induction kinetics at 3290 G following the induction of the new EPR signal dominating in Figure 1, spectrum d, during extended time (up to 4.5 min illumination). The kinetics shows that ca. 60% of the new EPR signal is formed in 10 s. EPR settings were the same as in Figure 1. For illumination conditions, see the text for details.

which did not visibly increase even during 4.5 min illumination (Figure 2B). Note that the spectra from Cyt b_{559} suffer from low signal-to-noise ratio. This is due to the low sample concentration in the flashed samples and that the spectra had to be acquired swiftly to avoid decay of any light-induced signals. Normally, the Cyt b_{559} spectrum requires long spectral accumulation time or very concentrated samples to record reasonable spectra, but this was not an option in our experiment. Our applied short and weak illumination at 5 K did not result in oxidation of Chl$_Z$ or Car while longer or stronger illumination at 5 K resulted in oxidation of narrow radical EPR signals from Car and/or Chl$_Z$ radicals. Representative EPR spectra are shown in Figure 2A. In the dark (Figure 2A, spectrum a), the radical region of the EPR spectrum only showed the signal from $Y_D^{\bullet}$ that was oxidized in all centers. When the samples were illuminated for 10 s at 5 K, the radical EPR spectrum did not change (Figure 2A, spectrum b). In contrast, when a longer illumination (4.5 min) with the same light intensity was applied, the EPR spectrum changed (Figure 2A, spectrum c). This change is due to buildup of a small, narrow radical in the middle part of the spectrum that is overlaid the broader spectrum from $Y_D^{\bullet}$. The pure radical spectrum (Figure 2A, spectrum d) can be obtained by subtraction of the dark spectrum (a) from the spectrum recorded after illumination (c).

This radical signal is similar to the signals from the Car and/or Chl$_Z$ radicals (52−56), and we assign our radical species to induction of one or both of these species. Thus, the experiment shown in Figure 2 shows that, during the first 10 s of illumination, no observable signals from other radical species are induced, accompanying the much broader EPR signals described in Figure 1. However, prolonged illumination resulted in oxidation of Car and/or Chl$_Z$, similar to what has been found before. After 4.5 min (Figure 2,

bottom) the radical was induced in approximately 10% of the PSII centers. This radical is stable at 5 K, which is consistent with previous reports (54). In large contrast to oxidation of this radical the new EPR signal described in Figure 1, spectrum d, was induced immediately upon the onset of the weak illumination. This is shown in the kinetic experiment presented in Figure 2C. Here, the induction at 3290 G of the broad EPR signal dominating in the 3-flash sample is followed during illumination up to 4.5 min. The signal is quickly induced; after 10 s (marked with an arrow, similar to the condition for spectrum b in Figure 2A) ca. 60% of the maximum amplitude is reached. The signal reaches maximum after ca. 2 min illumination, and with longer illumination the signal does not increase further. Consequently, the new signal is induced before and independently of the oxidation of the Car/Chl$_Z$ species.

All spectra and the kinetic in Figure 2 are recorded in 3-flash samples. However, we emphasize that the situation was similar in 0-flash samples (not shown). The short and weak illumination induced no detectable oxidation of Cyt b_{559} while a narrow radical from Chl$_Z$ or Car was induced only after several minutes of light exposure and then only to very limited (<10%) extent (not shown).

We tried to further establish if the split radical signals really oscillated with the S_1 and S_0 states. For this we used the S_2 multiline signal to quantify the S-state oscillation similar to what we have done earlier (43, 61, 62). Figure 3A shows how the intensity of the S_2 multiline signal (not shown) changes with the flash number. It clearly shows an oscillation with a period of four. On the basis of the amplitude of the signals in the 0-, 1-, 2-, and 5-flash samples, we can estimate the miss factor to about 16% in this particular experiment (the fit is shown with a dashed line in Figure 3A). This results in an S-state composition of ≈100%
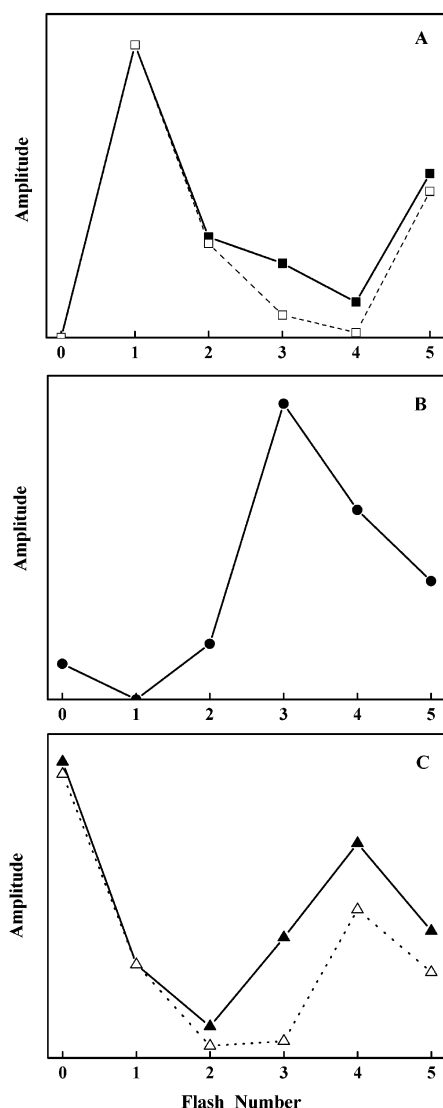
FIGURE 3: Oscillation of EPR signals in PSII samples given 0−5 flashes. (A) Oscillation of the S_2 state multiline EPR signal (filled squares). The intensity of the signal was estimated as in refs *43*, *61*, and *62*. From the S_2 multiline signal (spectra not shown) it was possible to estimate the approximate S-state composition in each sample (see text), and the simulation shown (open squares) was derived using 16% misses on each flash and a starting redox state containing 100% S_1 state and fully oxidized $Y_D^\bullet$. The error in the recorded S_2 multiline signal amplitude is ca. 5% when parallel samples are compared. (B) Oscillation with flash number of the relative intensity of the 160 G wide new EPR signal that is induced by illumination at 5 K. The signal is best visible in the 3-flash sample in Figure 1d. The intensity of the signal was estimated by its amplitude at 3260 G where the overlap is minimal with the more narrow signal (Figure 1a). The error in this measurement is larger (see text for explanation) than in the measurement of the multiline signal and of the signal recorded in the S_1 state. We estimate the error to be 10% when multiple parallel samples were compared. (C) Oscillation of the narrow (80 G wide) EPR signal inducible by illumination at 5 K, best observable in the 0-flash sample in Figure 1a. The solid line shows how the intensity measured at 3310 G varies with flash number. The amplitude at this field position is clearly a mix of the two signals in the 4- and 5-flash samples. The dashed line shows how the intensity difference, obtained by subtracting the intensity at 3260 G from the intensity at 3310 G, varies with flash number. This subtraction allows estimation of the narrow new signal with almost no interference from the broad signal (see text for explanation). The error in the measurement of this signal is ca. 5−10% between parallel samples, being less precise in the 4-flash sample when the signal is mixed with the signal dominating in the 3-flash sample.

S_1 state in the 0-flash sample; about 84% S_2 state and 16% S_1 state in the 1-flash sample; and 70% S_3 state, 27% S_2 state, and close to zero S_1 state in the 2-flash sample. In the 3-flash sample, there is about 60% S_0, 33% S_3, and 7% S_2 state; the 4-flash sample has about 50% S_1, 37% S_0, and 11% S_3 state. Finally, the 5-flash sample contained about 39% S_1, 15% S_0, 42% S_2, and 3% S_3 state.

Figure 3B shows the intensity changes at 3260 G of the broad split signal dominating in the 3-flash sample (see Figure 1d), as a function of flash number. The shoulder position (3260 G) of the broad split signal was chosen to avoid overlap with the narrow split signal (see Figure 1a) which is obvious in, for example, the 1- and 4-flash spectra. However, since we chose to measure outside of the maximum amplitude of the signal, the error in this measurement is larger than in the measurement of the multiline signal and of the signal recorded in the S_1 state. We estimate the error to be 10% when multiple parallel samples were compared. The 0-, 1-, and 2-flash samples give little or no absorption. The broad split signal comes and is maximal in the 3-flash sample. Here the S_0 state dominates. When one or two more flashes (4- and 5-flash samples) were applied, the intensity of the signal decreases again. In the 4-flash sample, the amplitude is a little more than half of that in the 3-flash sample while it is even smaller in the 5-flash sample. This correlates quite well with the oscillation of the S_0 state from 60% of the centers in the 3-flash sample to 37% and 15% in the 4-flash and 5-flash samples, respectively. We can deduce that the broad split signal arises from the PSII centers that were in the S_0 state. The very low amplitude in the 0-flash sample probably is due to a small fraction of centers still being in the S_0 state after the preflash. What seems to be a small amplitude in the 2-flash sample indicated in Figure 3B probably represents another signal (marked with an asterisk; see below) than the S_0 related signal.

Figure 3C shows the oscillation of the amplitude of the narrow split signal at 3310 G (solid line). However, the broad split signal present in the 3-, 4-, and 5-flash samples also contributes to the absorption at 3310 G. We note that the broad split signal (which is quite "clean" in Figure 1d) has almost the same absorption at 3310 and 3260 G. Therefore, the real oscillation curve of the narrow signal can be obtained by subtracting an intensity equal to the absorption at 3260 G of the broad split signal from the absorption at 3310 G. This gives rise to the "true" oscillation of the narrow signal and is presented as the dashed curve in Figure 2C. It is clear from Figure 3C (dashed curve) that the narrow EPR signal also has a period four oscillation pattern. The signal in the 0-flash sample has the highest amplitude, while the signal amplitude sequentially approaches zero in the 2- and 3-flash samples. The signal then comes back and reaches the second highest amplitude in the 4-flash sample. In the 4-flash sample, the signal is almost half of that in the 0-flash sample. This fits quite well with the S_1 state populations (100% in the 0-flash sample and 50% in the 4-flash sample).

In the 2-flash sample, containing about 70% S_3 and 27% S_2 centers, we observe no induction of split signals at all. This indicates that the illumination at 5 K of the S_2 and S_3 state centers could not result in the formation of redox states giving rise to split signals of this type. Note that in the 2-flash sample there is a signal at high magnetic field (3460 G) marked with an asterisk in Figure 1c, which is not present

in other samples. This signal is different from the signals in the S_0 and S_1 states and has not been assigned although it bears some resemblance to signals induced by near-infrared light in the S_3 state (*67*).

It was important to test whether the presence of the Mn cluster was necessary to induce these EPR signals. This was tested in Mn-deprived Tris-washed PSII membranes, but no split radical EPR signals of this type could be observed during illumination at 5 K in this material, indicating that the presence of the Mn cluster is necessary (not shown). We also tested whether illumination at 5 K of Ca^{2+}-depleted PSII samples frozen in the stable S_2 state resulted in formation of split EPR signals. Again, no split EPR signal could be observed (not shown).

Taken together, these results indicate that the formation of the oscillating split signals of this type at 5 K is strongly dependent on the S-states and the existence of the Mn cluster in PSII. Only the S_0 and S_1 states in the OEC can form split signals upon illumination at 5 K, and they give rise to two different split signals. In the S_1 state this signal has been observed before and assigned to magnetic interaction between the Mn cluster in the S_1 state and a nearby radical (either $Car^{+\bullet}$ or $Y_Z^{\bullet}$) (*57*).

Spectral Characteristics of the EPR Signals Induced by Illumination at 5 K. The spectra that we show in the flash series in Figure 1 are from a quite wide field region and contain a mix of EPR-detectable species in addition to the split radical EPR signals (see the discussion below about $Y_D^{\bullet}$ and the $Q_A^{-\bullet}Fe^{2+}$ signals). We therefore attempted to record "cleaner" spectra by the application of very high microwave power during the illumination procedure, leaving the new EPR signals nonsaturated (see below) while for example $Y_D^{\bullet}$ is quite saturated. The spectra are shown in Figure 4A. In the 0-flash sample, which is dominated by the S_1 state (spectrum a), the signal is clearly visible as a high, rather sharp peak on the low-field side of the $Y_D^{\bullet}$ spectrum. There is no corresponding peak on the high-field side of the $Y_D^{\bullet}$ spectrum. If the new signal is symmetric, the high-field peak should have appeared around 3390 G. This field position falls in the region where the $Y_D^{\bullet}$ spectrum totally dominates, despite the very high microwave power applied. It is therefore not possible at present to define the exact shape of the light-induced signal that we assigned to the S_1 state. However, the spectrum has a clear tailing at ca. 3410 G that indicates that it probably is a symmetric signal. In this case, it is only about 80 G wide, which is narrower than the split signals earlier observable from the donor side of PSII. It is, however, not possible to ascertain whether the signal is of the split radical type or if it is a broadened radical spectrum.

Spectrum b in Figure 4A was induced when the 3-flash sample (dominated by the S_0 state) was illuminated at 5 K. This spectrum is easy to resolve, due to the large width of the spectrum, which from peak to peak is about 160 G wide. Again, we cannot observe the middle part of the spectrum with precision enough to deduce if the signal is from a radical species that is split through magnetic interaction with a neighboring metal. However, the signal resembles earlier observed 100−160 G wide split radical signals from the $Y_Z^{\bullet}S_2$ state in Ca-depleted and other inhibited PSII (*24−44*). In the 3-flash sample the Mn cluster is not in the S_2 state as in earlier described split signals. Instead, we assign
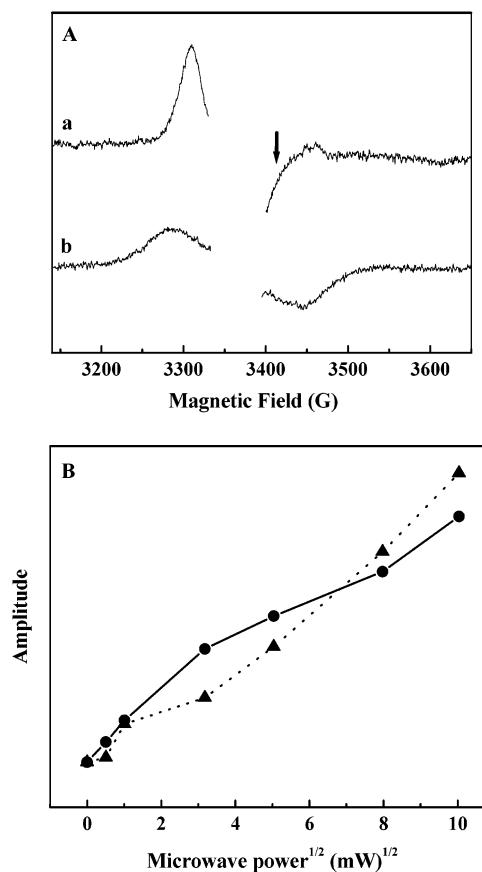

FIGURE 4: (A) Clean spectra of the split EPR signals from the 0-flash sample (spectrum a) and 3-flash sample (spectrum b). The spectra were recorded at 5 K at the very high microwave power of 100 mW. The spectra shown are the difference spectra between the spectra recorded during illumination at 5 K and spectra recorded in the same sample (0 flash or 3 flash) before the illumination. Other EPR settings are as in Figure 1. (B) Microwave power saturation at 5 K of the two split EPR signals. The amplitude of the narrow signal was estimated from the amplitude of the main peak at 3310 G in the 0-flash sample (dashed line), and the intensity of the broad signal was determined as the amplitude difference between the peak and the trough in a 3-flash sample (solid line). The EPR settings were as in Figure 1 except that the microwave power was varied.

the broad EPR signal inducible by illumination at 5 K to a magnetic interaction signal between the S_0 state and a close-lying radical on the donor side of PSII. By analogy we propose that the narrow signal in the 0-flash sample (Figure 4A a) originates from a radical in magnetic interaction with the S_1 state, a conclusion that is similar to the proposal put forward by Nugent et al. (*57*) from different data.

We also studied the microwave power saturation characteristics of the two signals. The results are shown in Figure 4B. At 5 K, both signals are impossible to saturate at microwave powers up to 100−150 mW. Above this power, the signals are difficult to detect with precision since the spectra tend to get very noisy at 5 K. Thus, both signals originate from very fast relaxing species, and in this respect they resemble the split radical signals from $Y_Z^{\bullet}S_2$ that relax very fast due to the interaction with the Mn cluster (*40, 52*). It is not possible to assign the radical that contributes to the spectra, but their fast relaxation does not provide any arguments against $Y_Z^{\bullet}$ as the radical in question.

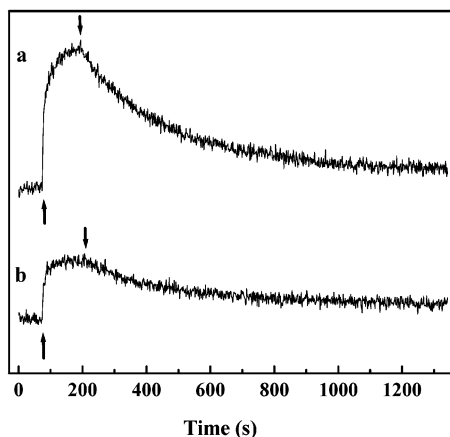*Kinetic Studies of the Induction and Decay of the New Signals.* We also investigated the lifetime in the dark of the

FIGURE 5: Induction and decay kinetics of the two split EPR signals at 5 K. The arrows indicate where the lamp was turned on (↑) and turned off (↓). The kinetic behavior of the split signal from the S_1 state was recorded by monitoring the EPR signal at 3310 G in the 0-flash sample (trace a). The kinetic behavior of the split signal from the S_0 state was recorded by monitoring the EPR signal at 3290 G in the 3-flash sample (trace b). The EPR settings were the same as in Figure 1. The spectral conversion time was 82 ms, and the time constant was 41 ms.

new signals. Our results are shown in Figure 5. The narrow split signal from the S_1 state is formed quickly to reach nearly its maximal extent by illumination for about 3 min. After 10 s of illumination (compare the conditions in Figure 2) more than half of the signal amplitude is induced. When the light is turned off, the signal from the 0-flash sample decays with a decay half-time of 214 s at 5 K (Figure 5, trace a). The signal from the S_0 state centers is a little more long-lived (Figure 5, trace b). Also this signal is induced quickly to more than 50% of its maximum amplitude after 10 s and to its maximal extent after about 3 min illumination. When the light is turned off, the signal decays slowly with a decay half-time of about 225 s.

The rise kinetics at 5 K of these split EPR signals (Figure 5) are sensitive to the exact illumination conditions (concentration of PSII, light intensity, etc.) since the formation of these split signals is very fast. Therefore, we could not obtain the real kinetics for the formation of these two EPR signals using continuous illumination. Instead, we investigated the flash-induced induction at 5 K of both signals to try to time resolve their formation. The results are shown in Figure 6. Samples given 0 (in the S_1 state) or 3 (in the S_0 state) flashes were given a weak laser flash (10−20 mJ) at 7 K. This resulted in a small and fast induction of the new split signals. To obtain interpretable kinetic traces, it was necessary to repeat the experiment in many samples, which is quite difficult at 7 K with high time resolution and high microwave powers. Therefore, the signal-to-noise ratio in our experiments is poor (Figure 6), but it nevertheless seems possible to approximately time resolve the induction of both signals. In both cases, the induction was complete within 20 ms after the flash. It seems that the induction half-time was about 10 ms or even faster, but this value is very uncertain due to the noise and the applied time constant (0.16 ms).

Crude Quantification of the Split EPR Signals That Are Induced at 5 K. Work with the $Y_Z^\bullet S_2$ signals has proven that exact quantification demands intimate knowledge of the participating spin systems and their magnetic interaction (*35,*
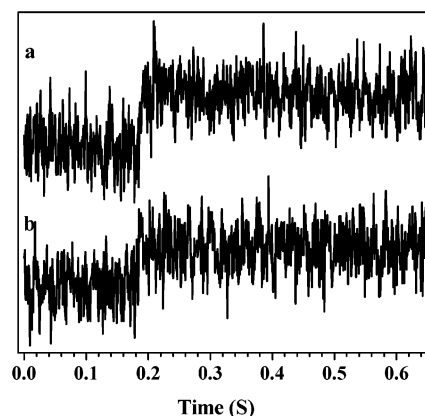

FIGURE 6: Time-resolved EPR measurements of the flash induction kinetics at 7 K of the two split EPR signals. Laser flashes (10−20 mJ) were provided directly into the EPR cavity at 7 K. The induction kinetics of the narrow split signal from the S_1 state was recorded by monitoring the EPR signal at 3310 G in the 0-flash sample (trace a). The induction kinetics of the broad split signal from the S_0 state was recorded by monitoring the EPR signal at 3290 G in the 3-flash sample (trace b). EPR conditions: temperature, 7 K; microwave frequency, 9.46 GHz; microwave power, 50 mW; modulation amplitude, 10 G; time constant, 0.16 ms. The kinetic traces shown are the average of four independent measurements in the same sample but performed with 30 min dark incubation at 7 K between the measurements to allow complete relaxation of the sample after each flash.

39, 40). It is too early at this stage to attempt such detailed theoretical analysis of our signals due to limited knowledge about the spin system in the Mn cluster in the S_0 and S_1 states.

Instead, we have attempted to obtain an idea of how many centers are involved in the formation of these signals by comparison with the amplitude of the split radical $Y_Z^\bullet S_2$ signals from Ca^{2+}-depleted PSII, which have large spectral resemblance (including overall spectral shape and microwave power saturation behavior) to the new signal induced in the S_0 state. We therefore compared the maximal signal size in a Ca^{2+}-depleted sample (not shown) with the maximal signal size in a 3-flash sample. We recorded the two signals at the same, unsaturated microwave power (10 mW) at 5 K (EPR conditions were the same as in Figure 1 except for the microwave power). Then we double integrated the parts of the spectra that lie outside the $Y_D^\bullet$ spectrum to obtain a comparable quantity of the signals. In our experiment, about 70% of the PSII centers gave the $Y_Z^\bullet S_2$ split signal in the Ca^{2+}-depleted PSII sample (not shown; see, however, ref *43* for a comparable analysis). Comparing the signal size between two such samples revealed that the new signal is induced in ca. 40 ± 4% of the available S_0 centers.

We used a similar method to quantify the PSII centers that give rise to the split EPR signal in the 0-flash sample. As discussed above, only part of this signal is clearly observable while a large part of the signal might be hidden under the spectrum from $Y_D^\bullet$. In our comparison we hypothesize that also this signal is symmetric and that the hidden half of the signal has the same area as the visible part. Then we compared the signal size to that in the Ca^{2+}-depleted sample. The rough calculation indicates that 14 ± 2% of the PSII centers in the 0-flash sample gave rise to the signal.

The conclusion we draw is that both signals originate from a large fraction of PSII. Thus, the signals represent an

important oxidation product on the donor side of PSII and not a negligible side path donor. In the case of the S_0 connected signal our crude analysis is probably not too erroneous since the most probable spin of the Mn cluster ($S = ^1/_2$) is similar to that in the S_2 state (*71–74*). In the case of the S_1 state connected signal, where the spin of the Mn cluster is less well characterized than in the S_0 state, we emphasize that our comparative analysis might be less informative than for the S_0 related signal. Nevertheless, our analysis indicates that both signals originate from significant fractions of PSII, which is in agreement with Nugent et al. (*57*), who found that the split signal in the S_1 state originated from a large fraction of the PSII centers.

DISCUSSION

Origin of the New EPR Signals. In this paper we have demonstrated two EPR signals that are generated by illumination at 5 K and that oscillate with the S-state of the OEC. One of the signals is connected to the S_1 state. This signal was first observed several years ago (*64*) and recently assigned to $Y_Z^\bullet$ or a Car radical in magnetic interaction with the Mn cluster in the S_1 state (*57*). The other signal is connected to the S_0 state and has not been described before. Both signals are formed efficiently already at low light intensities and rise within 10 ms after a laser flash. They are quite stable, and both decay in a few minutes in the dark.

Both signals are difficult to saturate with microwaves, and this fast relaxation, together with their overall spectral shape, indicates that they are split radical EPR signals that originate from magnetic interactions between a radical and a neighboring (ca. 10 Å away) metal center. Two sets of split signals have been reported from PSII. The split pheophytin signal (*68, 69*) originates from a magnetic interaction between reduced Pheo$^{-\bullet}$ and the nearby $Q_A^{-\bullet}Fe^{2+}$ center on the acceptor side of PSII. The other set of split signals was first discovered in Ca^{2+}-depleted PSII (*24, 25*) and was assigned to an organic radical in magnetic interaction with the Mn cluster. Analogous signals have been observed as a consequence of a variety of perturbations on the donor side of PSII, such as acetate inhibition (*33–42*), Ca depletion (*24–33*), high pH treatment of the S_3 state (*43*), or near-infrared illumination of the S_3 state (*67*). The signal in Ca^{2+}-depleted PSII was first assigned to a radical on a His residue close to the Mn cluster (*24, 25*), but the split signal was later found to originate from $Y_Z^\bullet$ in magnetic interaction with the S_2 state in acetate-treated PSII (*30*).

The formation of these two split signals is dependent on the presence of a functional Mn cluster. In addition, they show a four-period oscillation with flash number, which strongly argues for the Mn cluster (in the S_1 and S_0 states, respectively) being the metal center involved in the new signals.

An important question is the nature of the interacting radical and the nature of the magnetic interaction. The radical should be close to the Mn cluster and possible to photooxidize at 5 K. The redox chemistry on the donor side of PSII is very rich, and we know of many radical species close to the Mn cluster that can be formed by PSII photochemistry at extremely low temperatures (*49–56*). Possible candidates are $P_{680}^{+\bullet}$, $Chl_Z^{+\bullet}$, and $Car^{+\bullet}$, which are known to be functional at these temperatures. $Y_Z^\bullet$ and $Y_D^\bullet$ are also possible

candidates, and the latter was recently found to be photoinducible at 15 K at elevated pH (*70*). Less likely, but not impossible, is that the radical originates from another amino acid in the vicinity of the Mn cluster similar to what was originally proposed for the split signal in Ca^{2+}-depleted PSII (*24, 25, 28*). In the following we will provide our arguments for or against each of these candidates.

We do not favor $Y_D^\bullet$ or $P_{680}^{+\bullet}$ as the interacting partner. We still observe the signal from $Y_D^\bullet$ quantitatively as we observe the new signals (see Figure 2). It is thus not broadened by interaction with the S-states. Furthermore, $Y_D^\bullet$ is too far away (>30 Å) (*1, 2*) from the Mn cluster. This probably also holds for $P_{680}^{+\bullet}$, which has its spin centered more than 18 Å away from the Mn cluster (*1, 2*). There are also other arguments against $P_{680}^{+\bullet}$. We are not aware of reports of $P_{680}^{+\bullet}$ being stable for 5 min or more. Also, we do not observe any split signal in either S_2, S_3, or Mn-depleted or Ca^{2+}-depleted PSII during illumination at 5 K. In all cases, $P_{680}^{+\bullet}$ is likely to have been formed transiently, but we never observed it in our measurements. If it was that $P_{680}^{+\bullet}$ had existed for 5 min or more at 5 K in the S_1 and S_0 states, giving rise to the new EPR signals, it is likely to have existed for a long time also in some of the other samples. Thus, we can probably rule out $P_{680}^{+\bullet}$ as the radical partner to the Mn cluster.

We also do not favor $Chl_Z^{+\bullet}$ or $Car^{+\bullet}$ as the radical in our signals. Both Chl_Z and Car are known to be functional donors to $P_{680}^{+\bullet}$ at very low temperature. Many of these studies have been performed in PSII lacking the Mn cluster (*49–56*), and the situation in intact PSII is less clear. In our own measurements we have indeed observed formation of $Chl_Z^{+\bullet}$ or $Car^{+\bullet}$ during our illumination at 5 K of the flashed samples. However, the Chl_Z/Car radical is induced much later during the illumination than the split EPR signals we describe in this paper. This is clearly seen in Figures 2 and 5, where there is no induction of a narrow radical during the short (10 s) illumination that resulted in almost complete induction of the split signals (compare the induction kinetics in Figures 2C and 5) but substantial induction of narrow radicals during longer illumination (after 4.5 min) similar to what has been observed earlier (*52–56*). Furthermore, the induction of these radicals is not S-state dependent but occurs with rather similar kinetics irrespective of the S-state in the sample. Last, the radicals from Chl_Z/Car are quite stable and decay much slower at 5 K in the dark (many tens of minutes, not shown, and also see ref *54*) than the split signals (Figure 5), indicating that the signals are of completely different origin. Therefore, we rule out also Chl_Z and Car as the origin for the radical in the new signals. It is also likely that Chl_Z is situated too far away from the Mn cluster [the distance between the auxiliary chlorophylls and the Mn cluster is >20 Å as deduced from the X-ray structure (*1, 2*)] to give rise to signals of this kind.

We are thus left with either $Y_Z^\bullet$ or an unknown amino acid derived radical being formed by illumination at 5 K. At present, we cannot rule out an unknown amino acid. However, we prefer $Y_Z^\bullet$ from a few reasons. The main argument comes from the similarities between our signals and the extensively studied signal from $Y_Z^\bullet S_2$ in Ca^{2+}-depleted PSII. The signal in the S_0 state shows very similar overall spectral shape and low-temperature power saturation behavior to the $Y_Z^\bullet S_2$ in other Ca-depleted and acetate-treated

PSII (*24, 25, 39*). We therefore propose that it corresponds to the state $Y_Z^\bullet S_0$. The signal in the S_1 state is clearly different and much more narrow. The reported turnover experiment (*57*) suggests that the signal originates from $Y_Z^\bullet$ in magnetic interaction with the S_1 state.

Our results should be compared with those obtained from illumination at low temperature of Mn-depleted PSII or intact PSII. In most studies (*52−56*) the Car/Chl$_Z$/Cyt b_{559} pathway is oxidized with high yield by strong light ($10^2−10^3$ times higher than used here) and long illumination (e.g., $15−30$ min). We did not observe oxidation of these species by using short time (10 s) and weak light intensity illumination. This is consistent with the report of low yield of Car/Chl$_Z$/Cyt b_{559} oxidation by one saturating flash at low temperature (*54*). The integrity and function of the sample are also crucial, and the split signals are only formed in the S_1 and S_0 states; i.e., their formation demands a functional Mn cluster.

Taken together, these observations suggest that $Y_Z^\bullet$ is able to compete efficiently with the Car/Chl$_Z$/Cyt b_{559} pathway to give electron to P_{680}^+ in the S_0 and S_1 states. In many respects this is similar to the situation at elevated pH when Y_D was oxidized by a short illumination with weak light, while the apparent formation of Car/Chl$_Z$ radicals occurred only after prolonged illumination with strong light (*70*).

Implications for the Magnetic Properties of the Mn Cluster. Although the mechanism of the magnetic interaction behind the split signals is undefined, the mere existence of this type signal indicates that the Mn cluster is paramagnetic in the S_0 and S_1 states. The $g = 2$ multiline signal from $S = \frac{1}{2}$ of the Mn cluster in the S_0 state was reported a few years ago (*71−74*). However, this signal was only observed in the presence of methanol; the magnetic character of the S_0 state is still unclear without the presence of methanol. There are also EPR signals from integer spin states of the Mn cluster in S_1 state samples from PSII without the extrinsic subunits (23, 17 kDa) on the donor side (*59*) or from cyanobacteria (*75−77*). Our experiments are performed in intact PSII samples from higher plants without the presence of methanol where such EPR signals have not yet been found, suggesting that it might be worthwhile to intensify the search for signals also here.

Thus, the observation of the split signals reported here and in ref *57* provides new probes to investigate the properties of the S_0 and S_1 states in intact PSII. It indicates that the Mn cluster is paramagnetic in both the S_0 and S_1 states. The different width of the two signals might reflect differences in the spin features in the Mn cluster between the S_0 and S_1 states. Szalai et al. (*39*) found that the width of the $Y_Z^\bullet S_2$ split signals was sensitive to measurement conditions, e.g., temperature, which affected the magnetic interaction between the participating species. Thus, it is not feasible yet to distinguish the paramagnetic properties of the Mn cluster and the nature of the interaction between the radical and the Mn cluster. Further careful investigations, like the many detailed studies of the $Y_Z^\bullet S_2$ split signals (*39−42*), are needed.

Hydrogen-Bonding Properties of Y_Z. Oxidation of Y_Z results in formation of the deprotonated (neutral) form of the radical (*12, 13*). It is not obvious how $Y_Z^\bullet$ could be oxidized at temperatures as low as 5 K when the resulting $Y_Z^\bullet$ radical is deprotonated. This is because proton movements are severely restricted at 5 K (*78*).

We see two solutions to this dilemma. One is that Y_Z is already deprotonated in the reduced state. If this was the case, Y_Z oxidation involves no proton movement. Indeed, there exist optical spectroscopy results suggestive of a deprotonated Y_Z from the start of the reaction (*79*). However, there are also results obtained with the more telling FTIR technique that strongly indicate that Y_Z is H-bonded (*18, 19*). Thus, the experimental work on the protonation state of Y_Z is not unambiguous. There are also theoretical arguments against Y_Z being deprotonated in the reduced state. The redox potential in vitro of the Tyr$^\bullet$/Tyr$^-$ couple is only about 0.68 eV (vs NHE) (*80*), which is too low to allow water oxidation, which would require more than 0.82 eV at least. Therefore, we think it is unlikely that the normal working state of Y_Z would be the deprotonated form in the reduced state.

An alternative situation is that Y_Z forms a so-called *low-barrier hydrogen bond* (LBHB) or strong H-bond (*81*). It is known that protons cannot move in a normal (weak, such as in ice or water) H-bond at temperatures lower than 100 K (*78*). However, in case of the LBHB the interaction between the proton donor and the proton acceptor is much stronger. Theoretical studies reveal that the proton movement can occur even without overcoming the activation energy or only overcoming a small activation energy barrier (*82−84*). Consequently, the proton can move in the H-bond also at very low temperatures. LBHBs have been found in many enzymes systems, where they have crucial functions (*81, 85, 86*). In PSII, Y_Z is known to form a H-bond to a neighboring base (*14−19*), and site-directed mutants indicate that this base is D$_1$-His$_{190}$ (*12, 13*). However, the X-ray structure has not yet resolved this H-bonding partner(s) to Y_Z, and more work is needed to investigate the strong H-bond that we propose steers the function of Y_Z. In this respect we note that recent work (*70*) shows that also Y_D can be oxidized at 15 K at high pH. In the case of Y_D, one proposed explanation involves proton tunneling from Y_D to a neighboring base, D$_2$-His189 (analogous to D$_1$-His190). Thus, it seems that a strong H-bond to a close-lying His residue can indeed allow low-temperature oxidation of a tyrosine. Presumably, the situation is analogous around Y_Z.

Finally, we address why the oxidation of Y_Z was observed only in the S_0 and S_1 states but not in the S_2 and S_3 states. Optical spectroscopy revealed that the oxidation kinetics of Y_Z in the different S-states are slightly different at room temperature (*7, 87−89*), and the oxidation of Y_Z in the S_0 and S_1 states is easier than that in the S_2 and S_3 states. It is likely that ultra-low temperatures amplify this kinetic difference, making oxidation of Y_Z impossible in the higher S-states at 5 K. Our data provide little insight in the mechanism at present, but further studies of the low-temperature oxidation at different pHs and in various mutants will be most telling about the energetics involved in the interaction between the Mn cluster and its immediate environment including Y_Z.

REFERENCES

1. Zouni, A., Witt, H. T., Kern, J., Fromme, P., Krauss, N., Saenger, W., and Orth, P. (2001) *Nature 409*, 739−743.
2. Kamiya, N., and Shen, J. R. (2003) *Proc. Natl. Acad. Sci. U.S.A. 100*, 98−103.
3. Diner, B. A., and Babcock, G. T. (1996) in *Oxygenic Photosynthesis: The Light Reactions* (Ort, D. R., and Yocum, C. F., Eds.)

pp 213−247, Kluwer Academic Publishers, Dordrecht, The Netherlands.

4. Britt, R. D. (1996) in *Oxygenic Photosynthesis: The Light Reactions* (Ort, D. R., and Yocum, C. F., Eds.) pp 137−164. Kluwer Academic Publishers, Dordrecht, The Netherlands.

5. Rutherford, A. W., and Faller, P. (2001) *Trends Biochem. Sci. 26*, 341−344.

6. Nugent, J. H. A. (1996) *Eur. J. Biochem. 237*, 519−531.

7. Renger, G. (2001) *Biochim. Biophys. Acta 1503*, 210−228.

8. Debus, R. J. (1992) *Biochim. Biophys. Acta 1102*, 269−352.

9. Yachandra, V. K., Sauer, K., and Klein, M. P. (1996) *Chem. Rev. 96*, 2927−2950.

10. Dau, H., Iuzzolino, L., and Dittmer, J. (2001) *Biochim. Biophys. Acta 1503*, 24−39.

11. Stubbe, J., and van der Donk, W. A. (1998) *Chem. Rev. 98*, 705−762.

12. Debus, R. J. (2001) *Biochim. Biophys. Acta 1503*, 164−186.

13. Diner, B. A. (2001) *Biochim. Biophys. Acta 1503*, 147−163.

14. Svensson, B., Vass, I., Cedergren, E., and Styring, S. (1990) *EMBO J. 9*, 2051−2059.

15. Mamedov, F., Sayre, R. T., and Styring, S. (1998) *Biochemistry 37*, 14245−14256.

16. Hays, A. M. A., Vassiliev, I. R., Golbeck, J., H., and Debus, R. J. (1998) *Biochemistry 37*, 11352−11365.

17. Hays, A. M. A., Vassiliev, I. R., Golbeck, J. H., and Debus, R. J. (1999) *Biochemistry 38*, 11851−11865.

18. Berthomieu, C., Hienerwadel, R., Boussac, A., Breton, J., and Diner, B. A. (1998) *Biochemistry 37*, 10547−10554.

19. Noguchi, T., Inoue, Y., and Tang, X. S. (1997) *Biochemistry 36*, 14705−14711.

20. Svensson, B., Etchebest, C., Tuffery, P., Kan, P. V., Smith, J., and Styring, S. (1996) *Biochemistry 35*, 14486−14502.

21. Campbell, K. A., Peloquin, J. M., Diner, B. A., Tang, X. S., Chisholm, D. A., and Britt, R. D. (1997) *J. Am. Chem. Soc. 119*, 4787−4788.

22. Hienerwadel, R., Boussac, A., Breton, J., Diner, B. A., and Berthomieu, C. (1997) *Biochemistry 36*, 14712−14723.

23. Faller, P., Debus, R. J., Brettel, K., Sugiura, M., Rutherford, A. W., and Boussac, A. (2001) *Proc. Natl. Acad. Sci. U.S.A. 98*, 14368−14373.

24. Boussac, A., Zimmermann, J. L., Rutherford, A. W., and Lavergne, J. (1990) *Nature 347*, 303−306.

25. Boussac, A., Zimmermann, J. L., and Rutherford, A. W. (1989) *Biochemistry 28*, 8984−8989.

26. Sivaraja, M., Tso, J., and Dismukes, G. C. (1989) *Biochemistry 28*, 9459−9464.

27. Ono, T., and Inoue, Y. (1990) *Biochim. Biophys. Acta 1020*, 269−277.

28. Berthomieu, C, and Boussac, A. (1995) *Biochemistry 34*, 1541−1548.

29. Hallahan, B. J., Nugent, J. H. A., Warden, J. T., and Evans, M. C. W. (1992) *Biochemistry 31*, 4562−4573.

30. Gilchrist, M. L., Jr., Ball, J. A., Randall, D. W., and Britt, R. D. (1995) *Proc. Natl. Acad. Sci. U.S.A. 92*, 9545−9549.

31. Astashkin, A. V., Mino, H., Kawamori, A., and Ono, T. (1997) *Chem. Phys. Lett. 272*, 506−516.

32. Mino, H., Kawamori, A., and Ono, T. (2000) *Biochemistry 39*, 11034−11040.

33. Dorlet, P., Boussac, A., Rutherford, A. W., and Un, S. (1999) *J. Phys. Chem. B 103*, 10945−10954.

34. MacLachlan, D. J., and Nugent, J. H. A. (1993) *Biochemistry 32*, 9772−9780.

35. Szalai, V. A., and Brudvig, G. W. (1996) *Biochemistry 35*, 1946−1953.

36. MacLachlan, D. J., Nugent, J. H. A., Warden, J. T., and Evans, M. C. W. (1994) *Biochim. Biophys. Acta 1188*, 324−334.

37. Tang, X. S., Randall, D. W., Force, D. A., Diner, B. A., and Britt, R. D. (1996) *J. Am. Chem. Soc. 118*, 7638−7639.

38. Force, D. A., Randall, D. W., and Britt, R. D. (1997) *Biochemistry 36*, 12062−12070.

39. Szalai, V. A., Kuhne, H., Lakshmi, K. V., and Brudvig, G. W. (1998) *Biochemistry 37*, 13594−13603.

40. Lakshmi, K. V., Eaton, S. S., Eaton, G. R., Frank, H. A., and Brudvig, G. W. (1998) *J. Phys. Chem. B 102*, 8327−8335.

41. Peloquin, J. M., Campbell, K. A., and Britt, R. D. (1998) *J. Am. Chem. Soc. 120*, 6840−6841.

42. Dorlet, P., Valentin, M. D., Babcock, G. T., and McCracken, J. L. (1998) *J. Phys. Chem. B 102*, 8239−8247.

43. Geijer, P., Morvaridi, F., and Styring, S. (2001) *Biocehmistry 40*, 10881−10891.

44. Andréasson, L. E., and Lindberg, K. (1992) *Biochim. Biophys. Acta 1100*, 177−183.

45. Meulen, K. A. V., Hobson, A., and Yocum, C. F. (2002) *Biochemistry 41*, 958−966.

46. Styring, S., and Rutherford, A. W. (1988) *Biochim. Biophys. Acta 933*, 378−387.

47. Koike, H., and Inoue, Y. (1987) in *Progress in Photosynthesis Research* (Biggen, J., Ed.) Vol. 1, pp 645−648, Martinus Nijhoff, Dordrecht, The Netherlands.

48. Brudvig, G. W., Casey, J. L., and Sauer, K. (1983) *Biochim. Biophys. Acta 723*, 366−371.

49. Mathis, P., and Vermeglio, A. (1975) *Biochim. Biophys. Acta 369*, 371−381.

50. Noguchi, T., Mitsuka, T., and Inoue, Y. (1994) *FEBS Lett. 356*, 179−182.

51. Hillmann, B., and Schlodder, E. (1995) *Biochim. Biophys. Acta 1231*, 76−88.

52. Stewart, D. H., Cua, A., Chisholm, D. A., Diner, B. A., Bocian, D. F., and Brudvig, G. W. (1998) *Biochemistry 37*, 10040−10046.

53. Vrettos, J. S., Stewart, D. H., de Paula, J. C., and Brudvig, G. W. (1999) *J. Phys. Chem. B 103*, 6403−6406.

54. Tracewell, C. A., Cua, A., Stewart, D. H., Bocian, D. F., and Brudvig, G. W. (2001) *Biochemistry 40*, 193−203.

55. Hanley, J., Deligiannakis, Y., Pascal, A., Faller, P., and Rutherford, A. W. (1999) *Biochemistry 38*, 8189−8195.

56. Faller, P., Pascal, A., and Rutherford, A. W. (2001) *Biochemistry 40*, 6431−6440.

57. Nugent, J. H. A., Muhiuddin, I. P., and Evans, M. C. W. (2002) *Biochemistry 41*, 4117−4126.

58. Berthold, D. A., Babcock, G. T., and Yocum, C. F. (1981) *FEBS Lett. 134*, 231−234.

59. Campbell, K. A., Gregor, W., Pham, D. P., Peloquin, J. M., Debus, R. J., and Britt, R. D. (1998) *Biochemistry 37*, 5039−5045.

60. Arnon, D. I. (1949) *Plant Physiol. 24*, 1−15.

61. Styring, S., and Rutherford, A. W. (1988) *Biochemistry 27*, 4915−4923.

62. Bernat, G., Morvaridi, F., Feyziyev, Y., and Styring, S. (2002) *Biochemistry 41*, 5830−5843.

63. Yocum, C. F., Yerkes, C. T., Blankenship, R. E., Sharp, R. R., and Babcock, G. T. (1981) *Proc. Natl. Acad. Sci. U.S.A. 78*, 7507−7511.

64. Nugent, J. H. A., and Evans, M. C. W. (1998) in *Photosynthesis: Mechanisms and Effects* (Garab, G., Ed.) Vol. II, pp 1379−1382, Kluwer Academic Publishers, Dordrecht, The Netherlands.

65. Miller, A. F., and Brudvig, G. W. (1991) *Biochim. Biophys. Acta 1056*, 1−18.

66. Zimmermann, J. L., and Rutherford, A. W. (1986) *Biochim. Biophys. Acta 851*, 416−423.

67. Ioannidis, N., and Petrouleas. V. (2000) *Biochemistry 39*, 5246−5254.

68. Klimov, V. V., Dolan, E., Shaw, E. R., and Ke, B. (1980) *Proc. Natl. Acad. Sci. U.S.A. 77*, 7227−7231.

69. Rutherford, A. W., and Zimmermann, J. L. (1984) *Biochim. Biophys. Acta 767*, 168−175.

70. Faller, P., Rutherford, A. W., and Debus, R. J. (2002) *Biochemistry 41*, 12914−12920.

71. Åhrling, K. A., Peterson, S., and Styring, S. (1997) *Biochemistry 36*, 13148−13152.

72. Åhrling, K. A., Peterson, S., and Styring, S. (1998) *Biochemistry 37*, 8115−8120.

73. Messinger, J., Nugent, J. H. A., and Evans, M. C. W. (1997) *Biochemistry 36*, 11055−11060.

74. Messinger, J., Robblee, J. H., Yu, W. O., Sauer, K., Yachandra, V. K., and Klein, M. P. (1997) *J. Am. Chem. Soc. 119*, 11349−11350.

75. Dexheimer, S. L., and Klein, M. P. (1992) *J. Am. Chem. Soc. 114*, 2821−2826.

76. Yamauchi, T., Mino, H., Matsukawa, T., Kawamori, A., and Ono, T. (1997) *Biochemistry 36*, 7520−7526.

77. Campbell, K. A., Peloquin, J. M., Pham, D. P., Debus, R. J., and Britt, R. D. (1998) *J. Am. Chem. Soc. 120*, 447−448.

78. Cowin, J. P., Tsekouras, A. A., Iedema, M. J., Wu, K., and Ellison, G. B. (1999) *Nature 398*, 405−407.

79. Candeias, L. P., Turconi, S., and Nugent, J. H. A. (1998) *Biochim. Biophys. Acta 1363*, 1−5.

80. Tommos, C., and Babcock, G. T. (2000) *Biochim. Biophys. Acta 1458*, 199−219.

81. Cleland, W. W., and Kreevoy, M. M. (1994) *Science 264*, 1887−1890.

82. Borgis, D., and Hynes, J. T. (1996) *J. Phys. Chem. 100*, 1118−1128.

83. Cukier, R. I. (1999) *J. Phys. Chem. A 103*, 5989−5995.

84. Krishtalik, L. I. (2000) *Biochim. Biophys. Acta 1458*, 6−27.

85. Frey, P. A. (2001) *Magn. Reson. Chem. 39*, S190−S198.

86. Cleland, W. W., Frey, P A., and Gerlt, J A. (1998) *J. Biol. Chem. 273*, 25529−25532.

87. Brettel, K., Schlodder, E., and Witt, H. T. (1984) *Biochim. Biophys. Acta 766*, 403−415.

88. Jeans, C., Schilstra, M. J., and Klug, D. R. (2002) *Biochemistry 41*, 5015−5023.

89. Eckert, H. J., and Renger, G. (1988) *FEBS Lett. 236*, 425−431.